International Journal of Progressive Sciences and Technologies (IJPSAT)
ISSN: 2509-0119.

Vol. 38 No. 1 April 2023, pp. 84-92

Development of Total Suspended Solid (TSS) Estimation Algorithm Using Landsat 9 Satellite Imagery in Cacaban Reservoir Waters

Abdi Sukmono, Arief Laila Nugraha, Arwan Putra Wijaya, Resi Ahdityas

Department of Geodetic Engineering, Faculty of Engineering, Diponegoro University, Semarang, Indonesia

Email : sukmono35@gmail.com or abdisukmono@lecturer.undip.ac.id

***Abstract*—Landsat 9 imagery is an advanced development of the Landsat satellite imagery program. Since it began operating, the Landsat satellite program has been able to map areas both on land and water. The use of remote sensing methods is an efficient method for monitoring water areas. Various approaches have been made to obtain a more accurate method for extracting information about the waters by utilizing satellite imagery. One of the parameters that is often extracted is the distribution of Total Suspended Solid (TSS) parameters in waters. Dynamic changes and different water characteristics cause several available water TSS parameter algorithms to have less than optimal results in other water areas. This study aims to develop an empirical TSS algorithm model that is suitable for the waters of the Cacaban Reservoir by utilizing the correlation between image spectral values and in situ TSS values. The best regression model developed for estimating TSS values is found in the linear regression model with channel ratios 3 and 4. The coefficient of determination for the model is 0.819, RMSE 1.793 mg/L and NMAE 13.1%. The TSS distribution results in the Cacaban Reservoir on 24 May 2022 had a TSS range from 1.13 mg/L to 69.53 mg/L.**

Keywords*— *Algorithm, Landsat 9 imagery, Reservoir Waters, Total Suspended Solid

I. INTRODUCTION

The main problem of Cacaban Reservoir since it began operating in 1958 is the high level of sedimentation. Sedimentation that occurred even caused the capacity of the reservoir to shrink from 90 million m^3 to only 55 million m^3 left [1]. Human activities also play a role in increasing sedimentation. Reservoirs that receive water pollution loads exceeding their carrying capacity can cause a decrease in water quality. Water pollution is a very important problem to pay attention to, because water is needed in life.

One of the effective methods used to monitor the quality of reservoir waters and their distribution is to use remote sensing. Utilization of remote sensing using spectral characteristics obtained from image recording results is able to identify and analyze water quality parameters [2]. The parameter that is often used in monitoring the quality of a waters using remote sensing methods is Total Suspended Solid (TSS) [3]–[5]. Estimation of water quality parameters such as Total Suspended Solid (TSS) concentrations from satellite imagery is highly dependent on the accuracy of atmospheric corrections and water quality parameter algorithm models [6]. The study of atmospheric correction requires a comprehensive and rigorous study, so this research only focuses on developing water quality parameter algorithms. Several models of water quality estimation algorithms have been developed, as was done in Poteran waters, Madura [3]; on the coast of Berau waters [7]; in Kendari waters [8] and in Rawa Pening [9]. Changes in dynamic water conditions and different water characteristics have resulted in several available water quality parameter algorithms having less than optimal results in other water areas. Development of an algorithm for estimating the

Corresponding Author: Abdi Sukmono

concentration of TSS parameters by relying on image spectral values and in situ data is needed in order to obtain an estimation model that is suitable for the characteristics of the waters [3]. This research is expected to contribute to observing and identifying TSS parameters in the waters of the Cacaban Reservoir.

II. Materials And Methods

A. Research Location and Data

The scope of the area in this study is the tourism area of the Cacaban Reservoir which is located in Tegal Regency. Administratively, the Cacaban Reservoir is included in three sub-districts, namely parts of the Kedung Banteng sub-district, Jatinegara sub-district and Pangkah sub-district. The rivers that are the source of water for the Cacaban reservoir consist of several rivers such as the Cacaban river, the Curihagung river, the Kedondong river, the Menyawak river and about 35 of its tributaries. The Cacaban Reservoir Dam has a peak elevation of +80.5 m with a normal water level of +77.5m. The water capacity of the reservoir is about 57,000,000 m^3 with a catchment area of 59 km^2. The topographic appearance around the Cacaban Reservoir is in the form of wavy to hilly plains with varying heights (85 - 600 meters above sea level) [10]. The condition and area of the reservoir are suitable for estimating TSS using remote sensing methods. Regarding the location and appearance of the Cacaban reservoir can be seen at Figure 1.

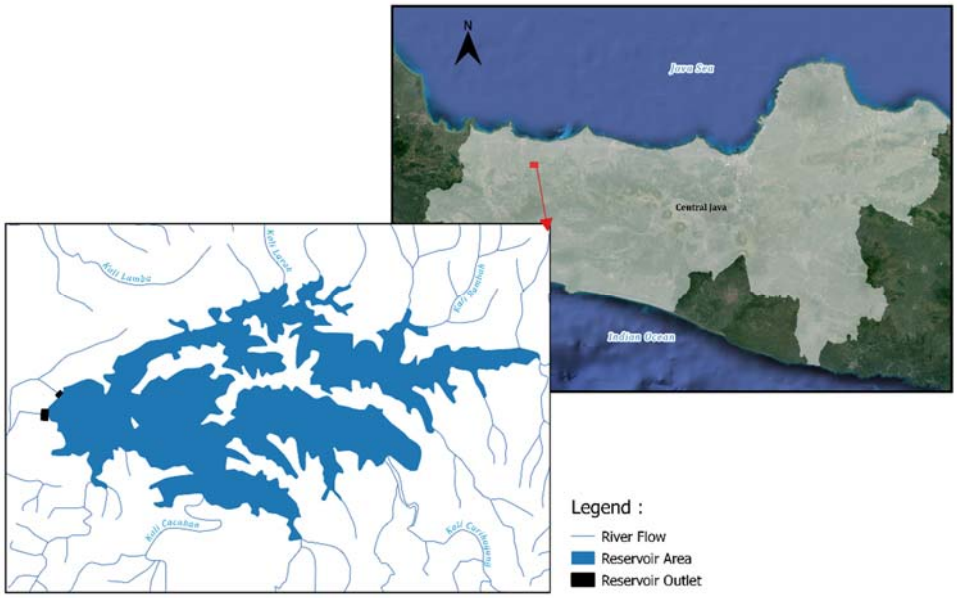

Fig. 1.Cacaban Reservoir as research area

The data used in processing this research are:

a. TSS in situ data for May 24, 2022 obtained from laboratory test results of reservoir water samples.

b. Landsat imagery 9 level L1TP path 120/row 65 recorded on May 24, 2022 which was downloaded free of charge via the USGS website.

c. Topographic map of Tegal Regency with scale of 1:25,000 which is used to test the geometric accuracy of the image.

B. Landsat 9 imagery Processing

Landsat 9 level L1 TP requires image preprocessing in the form of information being extracted before. This process is a radiometric correction. It is a correction made for errors found in sensors and sensor systems against detector responses and atmospheric influences. Radiometric correction is carried out in two stages, namely the radiometric calibration stage and the atmospheric correction stage. Radiometric calibration aims to convert image data that is still stored in the Digital Number (DN) into radiance and/or reflectance [6]. Atmospheric correction aims to convert the resulting data from radiometric calibration in the form of sensor reflectance (Top of Atmosphere reflectance) to surface reflectance (Bottom of Atmosphere reflectance). FLAASH

(Fast Line of-sight Atmospheric Analysis of Spectral Hypercub) method was used for atmospheric correction of Landsat 9. The FLAASH method uses the MODTRAN4 model and requires additional parameters that must be considered such as latitude longitude coordinates, sensor height, object surface height, date and time of recording of satellite image data, atmospheric models, aerosol models and visibility. [11].

The radiometric calibration stage makes the digital number values in pixels converted to radians or reflectance. Radiometric calibration is adjusted with FLAASH Settings. The output of the radiometric calibration image is in the form of a radian type image with the Band Interleaved by Line (BIL) storage format. The next step is to carry out atmospheric corrections with the aim of reducing errors due to differences in sensors and atmospheric conditions. The Landsat image which is already a TOA image is then subjected to atmospheric correction using the FLAASH method. In this study using FLAASH atmospheric correction because it is more effective at removing atmospheric influences compared to other methods. The atmospheric model used in FLAASH is the standard atmospheric model from the MODTRAN4 method. Atmospheric correction in this study uses the rural aerosol model because aerosols in the study area are not affected by industry, the atmospheric model uses tropical because it is in an area with a tropical climate. The result of the atmospheric correction is a BOA (Bottom of Atmosphere) image which is considered free from errors due to atmospheric effects and is ready for use.

C. TSS Algorithm Development

The algorithm for the TSS parameter is obtained from the regression equation resulting from the relationship between the reflectance value of the image and the value of the in situ data [12]. Image reflectance values with field data at the same coordinates are correlated using regression equations with various forms (Linear, Exponential and Logarithmic), as shown in Figure 2 , so as to obtain an appropriate empirical model of estimation [13].

TABLE I. REGRESSION MODELS

Regression Models	**Model Form**
Regresi Linier	$y = a + bx$
Eksponesial	$y = a * \exp(bx)$
Logaritmik	$y = a * \ln(x) + b$

Explanation:

x = Modified remote sensing reflectance value (single band or ratio band).

y = Concentration of TSS values in situ.

The development of the algorithm model in this study aims to produce an algorithm model that can show the actual situation in the research area. The data used in the development of the algorithm model are water TSS in situ data and image reflectance value data. TSS in situ data was obtained by testing the TSS content of water samples taken from the field. The reflectance value used as the independent variable is a single channel and a ratio channel from channels 1 to 5 of the Landsat 9 imagery acquired on May 24, 2022. The image acquisition period is close to the water sampling period. It is intended that the TSS algorithm model has a good level of accuracy. The development of the algorithm model uses linear, exponential and logarithmic regression equations. The number of sample data used to create the algorithm model is 20 sample data and 5 test point data with a distribution as in Figure 2. Determination of the best model based on accuracy tests using RMSE and NMAE with 5 test points.

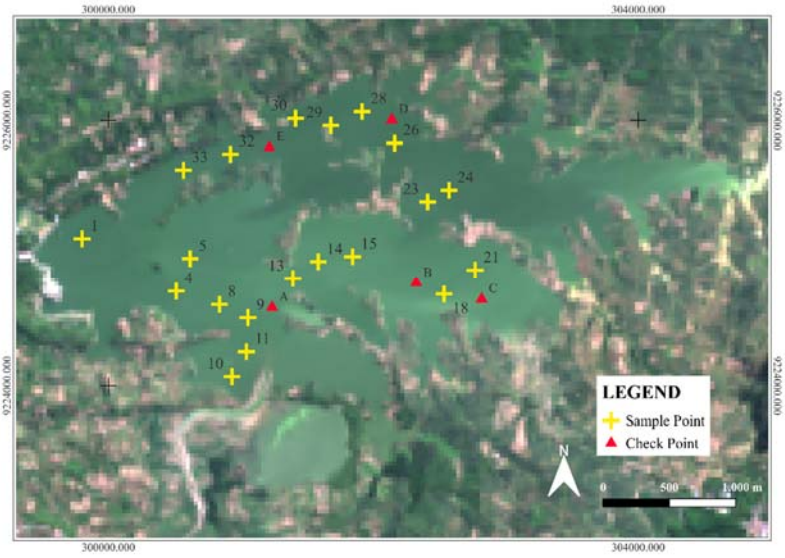

Fig. 2.Distribution of TSS Sample Points and Test Points

D. Accuracy Test

To test the accuracy of the image estimation results, the Root Mean Square Error (RMSE) and Normalized Mean Absolute Error (NMAE) tests are used according to equations (2.1) and (2.2). X_esti shows the results of in situ data measurements, while X_meas shows the results of image estimation results. Models with a coefficient of determination > 0.5, NMAE <30% and low RMSE show a good regression model in estimating [6].

$$\mathrm{RMSE} = \sqrt{\frac{\Sigma_{i=1}^{N}(X_{esti,i} - X_{meas,i})^2}{N}} \quad (1)$$

$$\mathrm{NMAE} = \frac{1}{N}\sum_{i=1}^{N}\left|\frac{X_{esti,i} - X_{meas,i}}{X_{meas}}\right| \times 100 \quad (2)$$

III. Result And Discussion

A. Radiometric Corection Result of Landsat 9 Imagery

The output of the radiometric calibration is a radian image in the BIL format. The atmospheric correction method used in this study uses the FLAASH Atmospheric Correction method. The FLAASH method is commonly used for images with multispectral to hyperspectral sensors. The input image used in the FLAASH method is a radiometric calibration image. The result of atmospheric correction using FLAASH is a Bottom of Atmosphere (BoA) reflectance image as shown in Table II.

The range of the reflectance value of the image that has been corrected for the atmosphere is at a reflectance value from 0 to 1 (average). In the results of this correction, the image has also been converted into .TIFF format, making it easier for further processing. The results of the atmospheric correction using the FLAASH method show the range of spectral values for each band between 0 and 1 as shown in Table II. Each channel has a minimum spectral range of 0 and a maximum of around 0.8.

TABLE II. LANDSAT 9 IMAGERY SURFACE REFLECTANCE VALUE ACQUISITION 24 MAY 2022

	Min	*Max*	*Mean*	*StdDev*
Band 1	0.000000	0.874900	0.054643	0.027227
Band 2	0.000000	0.817500	0.046786	0.026887
Band 3	0.000000	0.815000	0.068743	0.031297
Band 4	0.000000	0.818300	0.056286	0.032984
Band 5	0.000000	0.896000	0.231359	0.126260
Band 6	0.000000	0.860600	0.139527	0.079628
Band 7	0.000000	0.700400	0.070325	0.048091

B. TSS Model Agorithm Result

The equation model formed is the relationship between the in situ value as the Y (dependent) variable and the image spectral value as the X (independent) variable. Determination of the best algorithm that will be used to estimate the TSS value is taken based on the value of the coefficient of determination, RMSE and NMAE models. The results of the coefficient of determination in each model using a single band can be seen in Table III, as well as the band ratio on Table IV.

TABLE III. SINGLE BAND REGRESSION MODEL-COEFFIENT DETERMINATION (R^2)

Regression Models	**Single Band**				
	1	**2**	**3**	**4**	**5**
$y = a + bx$	0,000	0,0001	0,0036	0,0091	0,0258
$y = a * \exp(bx)$	0,000	0,0002	0,0038	0,0094	0,0258
$y = a * \ln(x) + b$	0,000	0,0003	0,0047	0,0080	0,0256

TABLE IV. RATIO BAND REGRESSION MODEL-COEFFIENT DETERMINATION (R^2)

Regression Models	**Ratio Band**									
	1/2	**1/3**	**1/4**	**1/5**	**2/3**	**2/4**	**2/5**	**3/4**	**3/5**	**4/5**
$y = a + bx$	0,002	0,016	0,026	0,026	0,042	0,132	0,015	**0,819**	0,021	0,0001
$y = a * \exp(bx)$	0,002	0,017	0,026	0,026	0,046	0,134	0,015	**0,790**	0,021	0,0001
$y = a * \ln(x) + b$	0,002	0,015	0,026	0,026	0,040	0,133	0,016	**0,817**	0,023	0,0002

Models with a coefficient of determination value greater than 0.5 are found in linear, exponential and logarithmic models of channel 3 and channel 4. To determine the accuracy of the model using the calculation of the RMSE and NMAE values of the 3 models at 5 test points located on Table V.

TABLE V. COEFFIENT DETERMINATION (R^2), RMSE AND NMAE 3 MODEL

Regression Models	Ratio Band 3/4		
	R^2	RMSE (mg/L)	NMAE (%)
$y = a + bx$	**0,819**	**1,793**	**13,10**
$y = a + bx^2 + b1x$	0,790	2,580	17,69
$y = a * \ln(x) + b$	0,817	1,802	13,16

Based on the coefficient of determination and accuracy test of 3 models on V, then it can be seen that the linear regression model of channel ratios 3 and 4 is the model with the best performance with an RMSE value of 1.793 mg/L, NMAE 13.1% and R^2 of 0.819. The regression plot can be seen in Figure 3.

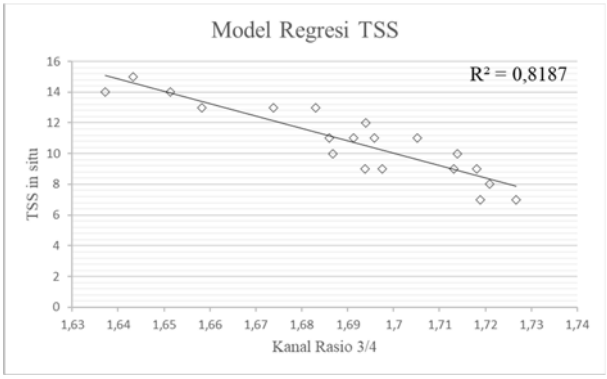

Fig. 3. Ratio of 3/4 bands linear regression plot for TSS estimation

The data plot points that form a regression line pattern from the bottom right up to the top left on Figure 3 shows the direction of a negative relationship between the independent and dependent variables. The linear regression model consists of the constants and regression coefficients of the independent variables.

	Sum of Squares	df	Mean Square	F	Sig.
Regression	86.130	1	86.130	81.296	.000
Residual	19.070	18	1.059		
Total	105.200	19			

The independent variable is Band34.

	Unstandardized Coefficients		Standardized Coefficients		
	B	Std. Error	Beta	t	Sig.
Band34	-80.802	8.962	-.905	-9.016	.000
(Constant)	147.390	15.151		9.728	.000

Fig. 4. Summary model of band ¾ linear regression

Figure 4 shows the summary of the results of the linear regression model with the in situ TSS value as the dependent variable and the ratio values of channel 3 and channel 4 as the independent variable. The calculated F value of the model is 81.296 with a significance level of 0.000 (<0.05) indicating that the regression model can be used to predict the TSS value. The model constant value is 147.39 and the regression coefficient value of the independent variables is -80.802. The value of the regression coefficient which is negative indicates the negative effect of the independent variable on the dependent variable. For every increase of one unit of the independent variable, the dependent variable will decrease by the value of the regression coefficient. Equation (3) shows the regression model of the TSS value and the channel 3 and channel 4 ratio values based on the constant parameter values and the regression coefficients contained in the summary model.

$$Y_{TSS} = 147{,}39 - 80{,}802 \times X_{\frac{B3}{B4}} \quad (3)$$

C. TSS Estimation Result From Landsat 9 Imagery Using Selected Algorithm

The distribution of TSS concentrations in Cacaban Reservoir waters on 24 May 2022 was obtained based on Landsat 9 imagery spectral data acquired on 24 May 2022 using the developed TSS algorithm model. The TSS distribution results in the Cacaban Reservoir on 24 May 2022 had a TSS range from 1.13 mg/L to 69.53 mg/L. TSS distribution was divided into 7 classes with the widest class area in the 10-20 mg/L class of 3,388,830 m^2 or 52.7% of the total water area. The narrowest area is 15,297 m^2 in the TSS class of 60-70 mg/L. TSS class ranges and their extent can be seen in Table VI.

TABLE VI. COEFFIENT DETERMINATION (R^2), RMSE AND NMAE 3 MODEL

No.	Class TSS (mg/L)	Area (m^2)	Precentage
1.	0-10	1.887.858	29,4%
2.	10-20	3.388.830	52,7%
3.	20-30	584.000	9,1%
4.	30-40	432.825	6,7%
5.	40-50	87.285	1,4%
6.	50-60	33.294	0,5%
7.	60-70	15.297	0,2%
Total		6.411.394	100%

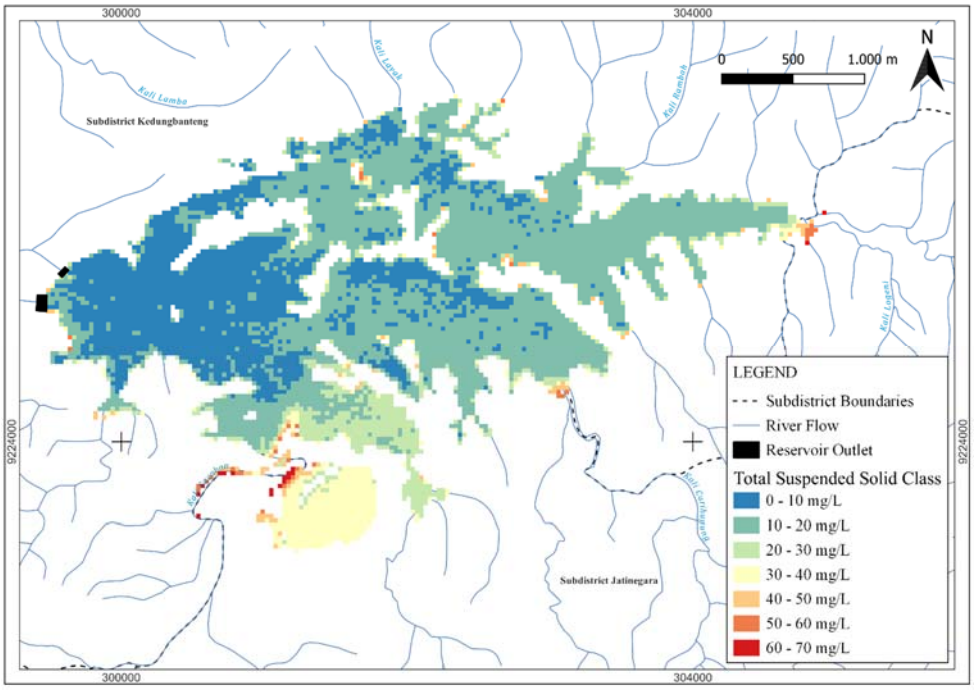

Fig. 5. Distribution of TSS concentrations in the Cacaban Reservoir on 24 May 2022

The results of mapping the distribution of TSS concentrations on Figure 4 shows that areas that have high levels of TSS concentrations are located in several parts of the mouth of the river that leads to the reservoir. This is because the river is a supplier of sediment and solids material, so that the TSS is high in the area around the river basin and lower in the middle of the reservoir/lake [14]. Based on observations from 2013 to 2022, the Cacaban River basin is an area with high concentrations of TSS. This condition is in accordance with the conditions of research conducted in the Cacaban watershed which has an average erosion of 99.74 tons/ha/year which is classified as a very high erosion rate. [15].

IV. Conclusion

The best regression model developed for estimating TSS values is found in the linear regression model with bandl ratios 3 and 4 as independent variables. The coefficient of determination for the model is 0.819, RMSE is 1.793 mg/L and NMAE is 13.1%. The coefficient of determination > 0.5 and NMAE <30% indicates that this model meets the requirements to be a TSS estimation model for Cacaban Reservoir waters. The TSS distribution results in the Cacaban Reservoir on 24 May 2022 had a TSS range from 1.13 mg/L to 69.53 mg/L. TSS distribution was divided into 7 classes with the widest class area in the 10-20 mg/L class of 3,388,830 m^2. The narrowest area is 15.297 m^2 in the TSS class of 60-70 mg/L

Acknowledgment

We are very grateful to Faculty of Engineering Diponegoro University for funding this research and publication through Strategic Research Scheme.

References

[1] W. Anggara and N. Sundari, " Study of "Study of Volume Changing of Cacaban Reservoir Using Echosounder Survey" - Studi Perubahan Volume Waduk Cacaban dengan Survei Pemeruman Waduk," J. Tek. Pengair., vol. 7, pp. 310–315, 2016.

[2] A. Sukmono, " Monitoring The Total Suspended Solid (TSS) of Gajah Mungkur Reservoir in 2013-2017 Using Landsat 8 imagery"-"Pemantauan total suspended solid (TSS) waduk Gajah Mungkur periode 2013-2017 dengan citra satelit landsat-8," J. Geod. dan Geomatika ELIPSOIDA, vol. 01, no. 01, pp. 33–38, 2018.

[3] N. Laili et al., "Development Of Water Quality Parameter Retrieval Algorithms For Estimating Total Suspended Solids and Chlorophyll-A Concentration Using Landsat-8 Imagery At Poteran Island Water," ISPRS Ann. Photogramm. Remote Sens. Spat. Inf. Sci., vol. 2, no. 2W2, pp. 55–62, 2015, doi: 10.5194/isprsannals-II-2-W2-55-2015.

[4] D. Heriza, A. Sukmono, and N. Bashit, " Water Quality Analysis of Rawa Pening Lake in 2013, 2015 and 2017 Using Multitemporal Landsat 8 Imagery"- "Analisis perubahan kualitas perairan Danau Rawa Pening periode 2013, 2015 dan 2017 dengan menggunakan data citra landsat 8 multitemporal," J. Geodesi. Undip, vol. 7, no. 1, pp. 79–89, 2018.

[5] L. M. Jaelani and R. Y. Ratnaningsih, "Spatial and temporal analysis of water quality parameter using sentinel-2A data; Case study: Lake Matano and Towuti," Int. J. Adv. Sci. Eng. Inf. Technol., vol. 8, no. 2, pp. 547–553, 2018, doi: 10.18517/ijaseit.8.2.4345.

[6] L. M. Jaelani, F. Setiawan, H. Wibowo, and Apip, "Chlorophyll-A Concentration Mapping Using Landsat 8 Imagery In Matano Lake and Towuti Lake, South Sulawesi" - "Pemetaan Distribusi Spasial Konsentrasi Klorofil-A dengan Landsat 8 di Danau Matano dan Danau Towuti , Sulawesi Selatan," Pertem. Ilm. Tah. Masy. Ahli Penginderaan Jauh Indones., no. XX, pp. 456–463, 2015, doi: 10.13140/RG.2.1.4278.6000.

[7] E. Parwati and A. D. Purwanto, "Time Series Analysis of Total Suspended Solid (Tss) Using Landsat Data in Berau Coastal Area, Indonesia," Int. J. Remote Sens. Earth Sci., vol. 14, no. 1, p. 61, 2017, doi: 10.30536/j.ijreses.2017.v14.a2676.

[8] M. A. P. Fanela, N. D. Takarina, and Supriatna, "Distribution of total suspended solids (TSS) and chlorophyll-a in Kendari Bay, Southeast Sulawesi," J. Phys. Conf. Ser., vol. 1217, no. 1, 2019, doi: 10.1088/1742-6596/1217/1/012150.

[9] E. Rachmadiana, B. Sasmito, and N. Bashit, "Analysis of Total Suspended Solid Changing Using Multitemporal Sentinel2-A Imagery (Study Case : Rawa Pening Lake, Central Java" - "Analisis Perubahan Konsentrasi Total Suspended Solid Secara Multitemporal Menggunakan Citra Sentinel 2A (Studi Kasus: Danau Rawa Pening, Jawa Tengah)," Jurnal Geodesi UNDIP Vol 12 no 01. April, pp. 1–4, 2022.

[10] A. Sumargo, "Appropriateness of Cacaban Reservoir utilization in the Development of Nature Tourism Areas in Tegal Regency" - "Kesesuaian Pemanfaatan Waduk Cacaban dalam Pengembangan Kawasan Wisata Alam di Kabupaten Tegal,". Thesis of Diponegoro University. 2006.

[11] L. Fibriawati, "SPOT-6 Atmospheric Corection Using MODTRAN Method"-"Koreksi Atmosfer Citra SPOT-6 Menggunakan Metode MODTRAN4," Semin. Nas. Penginderaan Jauh, pp. 98–104, 2016.

[12] P. Nurandani, I. S. Subiyanto, and B. Sasmito, "Mapping of Total Suspended Solid (TSS) Using Multi Temporal Satellite Imagery in Rawa Pening Lake, Central Java Province," Geod. Undip, vol. 2, pp. 72–84, 2013.

[13] M. D. Hermawan, B. Sasmito, H. Hani'ah, E. Parwati, and S. Budhiman, " Analysis of Total Suspended Matter and Chlorophyll-a Distribution Using Modis Level IB Imagery (Study Case : The Coastal of Pesawaran Regency) - "Analisis Distribusi Total Suspended Matter dan Klorofil-a Menggunakan Citra Terra Modis Level 1b (Studi Kasus Daerah Pesisir Kabupaten Pesawaran, Provinsi Lampung Tahun 2012)," J. Geod. Undip, vol. 2, no.1, pp. 1–15, 2013,

[14] N. Suwargana and D. Yudhatama, "Model of TSS and Brightness Measurement di Lake Waters Using SPOT-4 Satellite Imagery" - "Model Pengukuran Tss Dan Kecerahan Di Perairan Danau Menggunakan Citra Satelit Spot-4," Jurnal Segara vol. 4, pp. 390–402, 2014.

[15] H. Pramono, Study of Erosion and Sedimentation in the Cacaban Reservoir Watershed, Tegal Regency" "Kajian Erosi dan Sedimentasi pada DAS Waduk Cacaban Kabupaten Tegal," Thesis of Sultan Agung University. 2019.